Relativistic Runaway Electrons in TEXTOR-94

R. Jaspers 1), I.Entrop 1), K.H. Finken 2), N.J. Lopes Cardozo 1), H.L.M. Widdershoven 1,2).

1) FOM-Instituut voor Plasmafysica 'Rijnhuizen', Partner in the Trilateral Euregio Cluster, Association EURATOM-FOM, Postbus 1207, 3430 BE Nieuwegein, The Netherlands
2) Institut für Plasmaphysik, Partner in the Trilateral Euregio Cluster, Association EURATOM-KFA, Forschungszentrum Jülich GmbH, D-52425 Jülich, Germany

E-mail: r.jaspers@fz-juelich.de

Abstract. This paper reviews results concerning generation, confinement and transport of runaway electrons in the energy range 20-30 MeV in the TEXTOR tokamak. Runaway electrons above 20 MeV emit synchrotron radiation in the (near) infrared wavelength range, which can easily be detected by thermographic cameras. This technique is developed and exploited at the TEXTOR-94 tokamak and has resulted in some spectacular results. These include: the experimental evidence of the secondary ('knock-on') runaway generation; the discovery of the runaway snake; the observation of disruption generated runaways; the probing of magnetic turbulence in the core of the plasma in Ohmic and additionally heated plasmas.

1. Introduction

The phenomenon of electron runaway is an interesting and well-known result of the fact that the mean free path of an electron in a plasma is a strongly decreasing function of its velocity. In an electric field, electrons which exceed a critical velocity for which the collisional drag balances the acceleration by the field, are accelerated freely and can reach very high energies. Runaway electrons have been observed in nearly all tokamaks where they can reach energies of several tens of MeV's [1,2,3]. They are also encountered in other fields of plasma physics, e.g. in solar flares or thunderstorms [4].

The motivation for runaway electron studies in tokamak devices is twofold. First, for future fusion reactors, it is of major importance to know the processes of runaway generation and runaway loss during disruptions, because of the severe damage the local loss of large numbers of these highly energetic electrons may cause on first wall components [5]. Second, since the runaway electrons are effectively collisionless, their confinement is determined by the magnetic field turbulence. This fact can be used to probe the magnetic turbulence in the core of a thermonuclear plasma by measuring the confinement of runaway electrons.

Over the last decade, runaway studies have been performed at the medium sized tokamak TEXTOR (minor,major radius $a,R=0.46,1.75\ m$; typical plasma current $I_p=350\ kA$, magnetic field $B_t=2.25T$). These experiments where unique in the fact that the synchrotron radiation of relativistic electrons in the energy range 20-30 MeV was exploited for observing confined runaway electrons. These measurements yielded a wealth of information on runaway electron behaviour of which the highlights are reviewed in this paper.

2. Synchrotron Radiation

The synchrotron radiation is a powerful tool for the diagnosis the relativistic runaway electron distribution. This diagnostic provides a direct image of the runaway beam inside the plasma, recorded with a thermographic camera. From the spectral features the runaway energy can be obtained, the intensity of the radiation is a measure of the number of runaway electrons, and

A *B* *C*

Fig. 1. View into a low density TEXTOR-94 discharge with a thermographic camera looking into the direction of electron approach. In frame A recorded at t=0.5 s no synchrotron radiation is observable and only the wall structure can be recognized. In frame B, recorded at t=1.5s, the synchrotron radiation starts to develop and in frame C the full extent of the spot is visible from which the size of the runaway beam can be determined.

the synchrotron spot carries information on their perpendicular momentum and spatial distribution. Fig. 1 gives an example of such synchrotron measurement at TEXTOR-94 in the wavelength range 3-8 μm where the emission reaches its maximum. Detailed information on the synchrotron emission by relativistic electrons and the diagnostic can be found in Ref. [6].

3. Runaway Generation

Two mechanisms for the generation of runaway electrons are described by theory. The first, which we refer to as primary generation, treats the diffusion in velocity space of the electron distribution around the critical velocity. The production rate in this process depends exponentially on the parameter $\varepsilon=E/E_{crit}$, where E is the electric field and E_{crit} the field for which a thermal electron would run away: $E_{crit}\sim Z_{eff}n_e/T_e$. The second mechanism, secondary generation, is the process in which already existing high energetic electrons kick thermal electrons into the runaway regime by close Coulomb collisions. The production rate in this case is proportional to the number of runaway electrons and is therefore expected to lead to an exponential growth rate of the runaway generation. Because of this it is often referred to as the avalanche mechanism. Another important difference between the primary and secondary process is the very weak density dependence of the latter. The increased critical velocity at higher densities, which makes it more difficult for secondary electrons to reach the runaway region is compensated by the increased number of collisions. In a simplified treatment the secondary process can be parameterised by the avalanche time t_0, being the time in which an existing runaway electrons produces a new runaway electrons:

$$t_0[s]\approx 0.015\,(2+Z_{eff})/E[V/m].$$

If the runaway confinement time is longer than t_0 an exponentially increasing runaway population will be observed.

Predictions of runaway production during disruptions in future tokamak reactors are crucially dependent on the assumption whether or not the secondary generation dominates. However, the only experimental evidence for this process has been reported from TEXTOR [7]. This is illustrated most convincingly in Figure 2. Analysis of the time behaviour of the

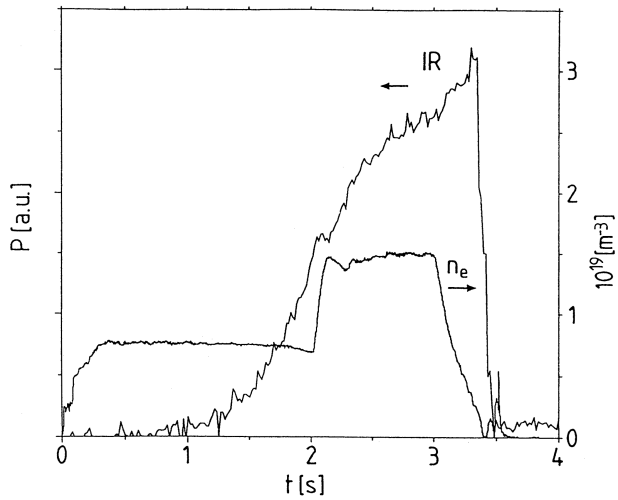

FIG. 2. Evidence for secondary generation on TEXTOR. Time trace of the infrared (IR) synchrotron radiation shows an exponentially increase and continues to increase when the density is doubled.

synchrotron radiation in low density ($n_e(0)\approx 1\times 10^{19} m^{-3}$) discharges showed the exponential increase and the weak density dependence expected for the avalanche mechanism. Note that for the case under consideration the synchrotron radiation signal is almost directly proportional to the number of confined runaway electrons.

4. Disruptions

In a few instances the generation of runaway electrons during major disruptions has been observed with the synchrotron radiation diagnostic on TEXTOR. An example was shown in Ref. [8]. There it is shown that there is a delay of a few ms between the thermal quench and the observation of non-thermal ECE radiation and a small beam of high energetic runaway electrons as witnessed by the synchrotron radiation. Probably, in the phase in between, the magnetic configuration was still stochastic, preventing runaway electrons to be confined long enough to reach high energies. Another observation made was that once the synchrotron radiation was observed the intensity did not increase further, irrespective of the high loop voltage measured. This indicates that in the centre of the plasma the runaway current was nearly as large as the plasma current before the disruption. Based on these observation a simple zero dimensional model was developed which described the TEXTOR data reasonably well by taking into account the secondary generation mechanism. One prediction of this study is that in a reactor, a **high** runaway generation rate during a disruption will prevent the runaway electrons from reaching high energies and so limits the damage, compared to a modest production rate. Nevertheless a complete suppression of the runaway generation will be favoured. Attempts to prevent runaway production by a huge Helium gas puff are being conducted at TEXTOR. Experiments show that it is possible to stop the runaway electrons in this way, and the helium injection offers other complimentary advantages such as the mitigation of the heat pulses released during a disruption by radiative cooling.

5. Runaway confinement in Ohmic discharges.

From the intensity distribution in the observed beam of synchrotron emission, the density profile of runaway electrons in the energy range 25-30 MeV could be derived. The source function was determined from the rate of increase of the signal during the period that secondary generation is not yet active. From these measurements the profile of the diffusion coefficient D_{ra} was derived. A typical value found at half radius was $D_{ra}\approx 0.01\ m^2/s$. This is consistent with a runaway confinement time of $\tau_{ra}\approx 3.5$ s. The latter figure is corroborated by the measurements of secondary generation, in which $\tau_{ra}\approx 0.8$ s is required to allow the exponential growth of the population. Thus, in Ohmic discharges, the runaway electrons confinement is excellent (for comparison, the energy confinement time is ≈ 0.03 s). As is shown below (Sec.6), runaway confinement inside magnetic islands is similarly good. The fact that the runaway confinement can be so good is attributed to the orbit shift of ~5 cm, which effectively decorrelates the runaway orbits from any turbulence with a radial correlation length shorter than that [11]. In Sec. 7 we show that this situation changes dramatically when high power additional heating is applied.

6. Runaway Snake

Relativistic runaway electrons are effectively collisionless, and their confinement is determined by the magnetic field structure. In the presence of macroscopic MHD modes in the plasma the magnetic configuration is drastically altered, and this is expected to have an effect on the runaway electrons. Therefore studies were made in low density runaway

discharges, in which MHD modes were excited by injection of a deuterium pellet. The result was rather spectacular [9]. The growth of the MHD modes after the injection resulted in the sudden loss of an appreciable part of the runaway population, with an effective diffusion coefficient of $D_{ra}\approx 300$ m^2/s. This fast loss was attributed to a temporary stochastisation of the magnetic field. The remaining runaways formed a narrow helical beam at the q=1 drift surface, as observed as small spots on the IR camera, see Fig. 3. The relation with the q=1 surface deduced from a) the positions of these synchrotron spots, b) the rotation frequency being equal to the m=1 magnetic perturbations and c) the angle β the major axis of the formed ellipse makes with the equatorial plane, which should be tan $\beta\approx D/qR_0$, D being the distance between observed runaway electrons and the detector [10]. The radial and poloidal diffusion of the beam is extremely slow ($D<0.02$ m^2/s). In some discharges, where the MHD activity was provoked not by pellet injection but by a plasma shift, even q=2 snakes could be observed. The fact that this so-called runaway snake persists after the rapid loss shows that there are still big remnant islands during the period of field stochastisation. The runaway electrons that are topologically associated with the O-point of the island survive the stochastisation, and remain very well confined. Interestingly, due to the orbit shift, they may physically live outside the magnetic island.

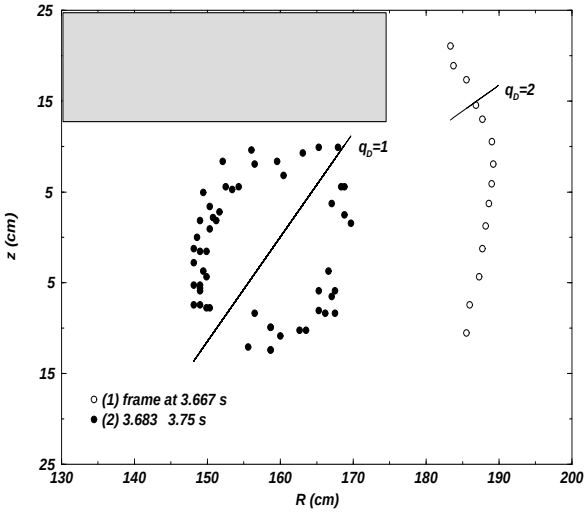

FIG.3. Centres of the spots of synchrotron radiation observed on successive frames of the IR camera. It is seen that they form an ellips whose major axis is inclined to the equatorial plane, proportional to the safety factor. A q=1 and q=2 runaway snake has been observed.

7. Probing turbulence with runaway electrons

One principal difficulty with the assessment of magnetic turbulence using relativistic runaway electrons, is that the orbits of these electrons are shifted with respect to the magnetic field topology by a few cm. This reduces the sensitivity to magnetic perturbations with radial correlation lengths smaller than this orbit shift [11]. Although this might seem a show stopper, it is exactly this effect which is utilised to estimate the correlation length of the turbulence [12], in experiments with additional neutral beam heating at TEXTOR.

Time traces of the synchrotron radiation in low density NBI heated discharges are depicted in Fig. 4. In the Ohmic phase the runaway confinement is excellent and the emission rises exponentially due to the secondary generation. During the NBI interval the infrared signal starts to decrease with a rate depending on the NBI power. Clearly the runaway confinement is deteriorated by the power input, which is expected since it is well known that confinement of heat and particles also degrades with increasing heating power. However, the decline of the runaway population does not start instantaneously after the heating is switched on, but is significantly delayed. It was shown in [12] that this delay is due to loss of runaway confinement at lower energies, which only later appears as reduced influx of observable runaway electrons at high energy. If there is a critical energy below which the runaway electrons are lost, the delay time is the time electrons at the critical energy need to be accelerated to the energy where they become observable. Thus, the delay time can be related to the critical energy, and so to the radial scale length of the magnetic turbulence.

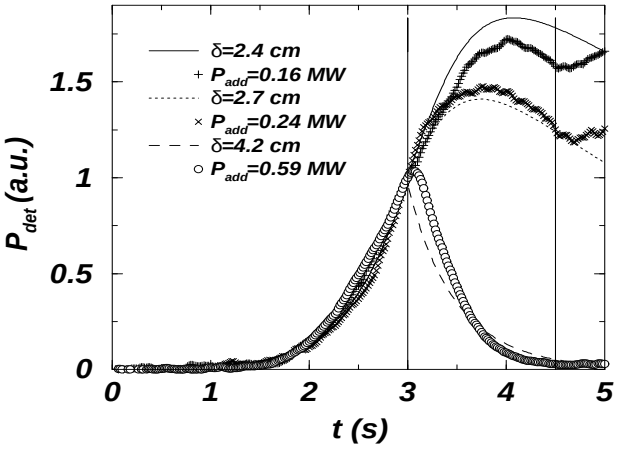

FIG. 4. Evolution of the runaway population of 20-30 MeV in discharges with additional heating by neutral beam injection from [3,4.5s]. When the heating is applied the signal drops, indicating loss of electrons due to magnetic turbulence. However, the marked delay in the response of the signal shows that the loss occurs at energies well below the 'visible' range (20-30 MeV). These data can be reproduced (thin lines) by a model having only a critical loss energy as free parameter. From this loss energy the scale size of the magnetic turbulence can be deduced.

Based on these observations simulations have been carried out with an energy dependent runaway confinement. The theory of Ref. [11] was adopted which gives a prescription of the transport reduction due to the orbit shift averaging. The only control parameter in this simulation is then the mode width δ. The results of the simulations are overlaid on the synchrotron radiation signals in Fig. 4. The derived correlation lengths for the NBI power scan are shown in Fig. 5. In the core of the plasma they amount to 0.2 cm in Ohmic discharges, increasing to several cm with 0.6 MW.

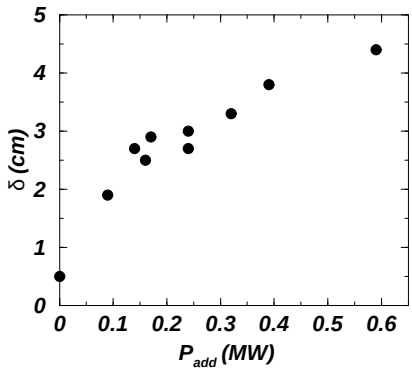

FIG. 5 Deduced mode width as a function of the NBI power.

8. Discussion

The synchrotron radiation diagnostic has proven to be a very powerful tool for studies of relativistic runaway electrons. Since there exists hardly any other method to measure the magnetic turbulence in the hot plasma core relativistic runaway electrons can improve our understanding of the transport processes in the plasma. Now it has been shown that even quantitative results can be obtained, although a more firm theoretical basis has to be developed. Apart from that, other interesting themes can be addressed by this method, such as the runaway behaviour in the presence of transport barriers, or the application of ergodic fields with external coils (using the TEXTOR Dynamic Ergodic Divertor [13], presently under construction).

References

[1] KNOEPFEL, H, SPONG, D.A., Nucl. Fusion **19** (1979) 785.
[2] GILL, R.D., Nucl. Fusion **40** (2000) 163.
[3] FINKEN, K.H. et al., Nucl Fusion **30** (1990) 859.
[4] GUREVICH, A.V. et al., Radio Science **31** (1996) 1541.
[5] PUTVINSKI, S. et al, Plasma Phys. Control. Fusion **39** (1997) B157.
[6] JASPERS, R. et al., Rev. Sci. Instrum. **72** (2001) accepted for publication.
[7] JASPERS, R. et al., Nucl Fusion **33** (1993) 1775.
[8] JASPERS, R. et al., Nucl. Fusion **36** (1996) 367.
[9] JASPERS, R. et al., Phys. Rev. Lett. **72** (1994) 4093, ENTROP, I. et al., Plasma Phys. Control. Fusion **41** (1999) 377.
[10] PANKRATOV, I.M. Plasma Phys. Reports **22** (1996) 535.
[11] MYNICK, H.E. and STRACHAN, J.D. Phys. Fluids **24** (1981) 695.
[12] ENTROP, I. et al., Phys. Rev. Lett. **84** (2000) 3606.
[13] FINKEN, K.H., Fusion Engineering and Design **37** (1995) 335-450.